New Journal of Physics
The open-access journal for physics

Hot electrons induced by slow multiply charged ions

T Peters[1], C Haake[1], D Diesing[2], D A Kovacs[3], A Golczewski[4], G Kowarik[4], F Aumayr[4], A Wucher[1] and M Schleberger[1,5]

[1] Experimentelle Physik, Universität Duisburg-Essen, 47048 Duisburg, Germany
[2] Physikalische Chemie, Universität Duisburg-Essen, 45117 Essen, Germany
[3] Experimentalphysik II, Ruhr-Universität Bochum, 44801 Bochum, Germany
[4] Institut für Allgemeine Physik, Technische Universität Wien, A-1040 Vienna, Austria
E-mail: marika.schleberger@uni-due.de

New Journal of Physics **10** (2008) 073019 (8pp)
Received 8 April 2008
Published 9 July 2008
Online at http://www.njp.org/
doi:10.1088/1367-2630/10/7/073019

Abstract. The dissipation of energy following the impact of multiply charged ions on a polycrystalline metal surface was studied using thin film metal–insulator–metal junctions as targets. The ions hit the top Ag layer of a Ag–AlO_x–Al junction, where they excite electrons and holes. A substantial fraction of these charge carriers is transported across the insulating barrier and can be detected as an internal current in the bottom Al layer. The effects of potential and kinetic energies on this tunneling yield are investigated separately by varying the charge state of the Ar projectile ions from 2+ to 8+ for kinetic energies in the range from 1 to 12 keV. Per impinging ion yields of typically 0.1–1 electrons are measured within the thin film tunnel junction. The tunneling yield is found to scale linearly with the potential energy of the projectile. In addition, the tunneling yield shows a strong dependence on the internal barrier height which can be modified by an external bias voltage.

The interaction between energetic ions and solid surfaces has been studied intensively in recent years. Ions may carry energy into the solid either as kinetic energy due to their velocity or as potential energy due to their charge state. In the case of slow ions (kinetic energy of a few kilo-electron-volt), the excitation of target electrons can be enhanced if multiply charged ions (MCI) are used [1, 2]. If such an MCI comes close enough to a metal surface, high lying Rydberg states of the projectile are resonantly filled with electrons from the conduction band of the metal. This so-called hollow atom [3] is neutralized and partially deexcites via multiple Auger transitions

[5] Author to whom any correspondence should be addressed.

while approaching the surface [4]–[6]. At perpendicular incidence the time available in front of the surface is too short for a complete relaxation of the projectile and thus the fraction of potential energy which is dissipated above the surface amounts to only 10% [7]. Within the solid the projectile still forms a hollow atom (although smaller [5]) which has retained most of its original potential energy. Subsequent charge transfer via Auger transitions continues inside the solid until complete deexcitation [8]. The mean deexcitation time within the solid is about 10 fs [9, 10] and therefore, the potential energy surviving the above-surface deexcitation processes is dissipated within the first few atomic layers.

Thus, the dissipation of the potential energy introduced by an MCI involves mainly Auger transitions which can be experimentally followed by measuring the corresponding electrons emitted from the solid into the vacuum (for an extensive review see [11]). A first attempt of a direct investigation of the excitation of hot charge carriers induced by a hollow atom *within* the solid was made by Schenkel *et al* [12]. In the present paper, we will show that the excitation can be detected by means of a thin film metal–insulator–metal (MIM) junction and that in this way complementary and hitherto inaccessible data for a different range of the ions, kinetic and potential energies can be obtained. In addition, the MIM can be applied as an energy dispersive element and more detailed information about the distribution of the electronic excitation after MCI impact can be obtained (see upper part of figure 4). These details will be discussed in the framework of a theoretical model in a separate paper [13].

The MIM junctions employed here consist of a 50 nm thick Al film covered by an AlO_x insulating layer of about 4 nm thickness formed by anodic oxidation, and a 20 nm thick silver film on top (see figure 1(b)). Further details of the preparation procedure can be found in [14]. The operation principle is illustrated in figure 1(b): between the two metals a bias voltage U_{bias} can be applied, such that for $U_{\mathrm{bias}} > 0$ the Ag film is on negative potential and for $U_{\mathrm{bias}} < 0$ on positive potential with respect to the aluminium film. The application of a bias voltage changes the detection characteristics of the MIM junction as discussed below.

The tunneling current I_{T} (see below) was measured using a current-to-voltage converter with a conversion factor of 10 mV pA^{-1}. The primary ion beam current I_0 was measured using a Faraday cup. The samples were bombarded under an angle of 90° (relative to the surface plane) with multiply charged Ar^{q+} ions with $q \leqslant 8$ produced by an electron cyclotron resonance (ECR) ion source of 14.5 GHz [15]. The ion beam was pulsed with a typical pulse width of 1.5 s. All experiments were performed under a typical background pressure of $p = 5 \times 10^{-8}$ mbar.

As a consequence of the ion deexcitation and neutralization processes occurring during irradiation, electrons are excited into empty levels of the conduction band of the exposed Ag film, each of them leaving behind one (excited) hole. Depending on the corresponding wave vector **k**, one excited carrier (electron or hole) is either emitted towards the surface or towards the Ag–AlO_x interface. Inelastic scattering processes along the trajectory of the carrier lead to energy loss and generation of further excited carriers. A charge carrier reaching the surface may escape into the vacuum only if it possesses enough kinetic energy to overcome the Ag–vacuum barrier. Thus, with an external detector only these electrons can be measured ('external emission') while holes meet an infinitely high potential barrier at the surface.

At the Ag–AlO_x interface the situation is very different. An electron can pass the potential barrier not only if its kinetic energy E_{kin} is larger than the barrier height Φ_{e}, but also if $E_{\mathrm{kin}} < \Phi_{\mathrm{e}}$, due to quantum mechanical tunneling. In addition, excited holes can pass the oxide, too, either via the valence band of the oxide or by tunneling through the barrier. As a result, both types of charge carriers can be detected in the Al film ('internal emission') as a net current

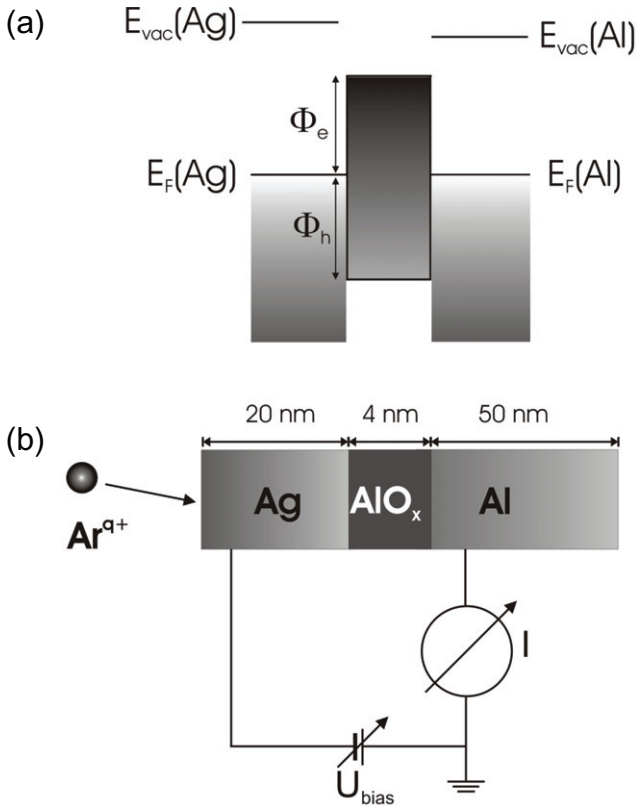

Figure 1. (a) Simplified energy diagram (zero bias voltage) of a Ag–AlO_x–Al junction. E_F(Ag) and E_F(Al) are the Fermi levels, whereas E_{vac}(Ag) and E_{vac}(Al) are the vacuum levels corresponding to Ag and Al, respectively. The potential barrier heights for electrons and holes are denoted by Φ_e and Φ_h. (b) Operation principle and sketch of a Ag–AlO_x–Al junction. I_T is the tunneling current and U_{bias} is the applied bias voltage; here $U_{bias} = 0$.

$I_T = |I_e| - |I_h| \neq 0$, which we will call in the following 'tunneling current'. Here, I_e and I_h designate the electron and the hole contributions to the tunneling current, respectively. The detection efficiency γ of a MIM device may be defined as the net number of electrons flowing between the Ag and the Al electrode per incident ion. This quantity we will call in the following 'tunneling yield', being given by $\gamma = I_T/(I_0/q)$.

Figure 2 shows the tunneling yield γ as a function of the potential energy E_{pot} for four kinetic impact energies. The data are plotted against the total potential energy stored in the projectile in the form of its ionization energy. The data recorded at 1, 4, 8 and 12 keV are well fitted by straight lines. This apparently linear behavior is in good agreement with previous measurements of the external electron emission yield γ_{ext} induced by Ar^{q+} ions with $q \leqslant 8$ at various metal surfaces [16]–[18]. For the projectiles investigated in this work the image charge acceleration observed at higher charge states [19, 20] can be neglected and the fluorescence yield is expected to be low [21]. Thus, the deexcitation happens mainly via Auger transitions. These Auger transitions lead to an electron emission which may be assumed to be isotropic. Consequently, electrons are emitted not only into the vacuum, but also towards the Ag–AlO_x interface where they may overcome the tunneling barrier with a mean height

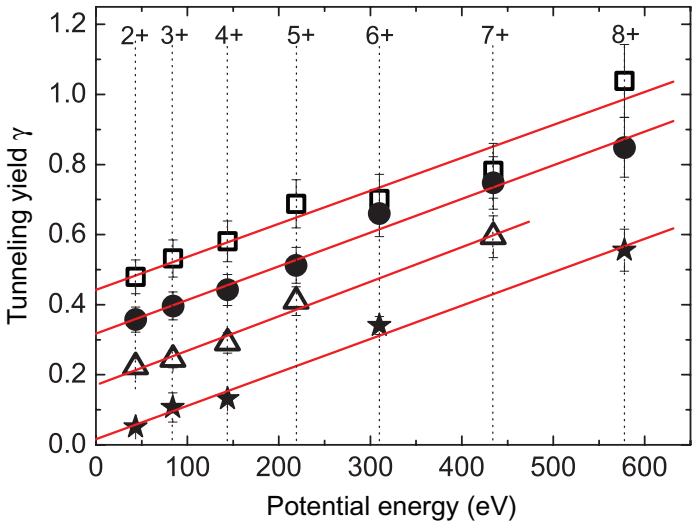

Figure 2. Tunneling yield γ as a function of potential energy measured for Ar projectiles with kinetic energies of 1 keV (stars), 4 keV (triangles), 8 keV (dots) and 12 keV (squares).

$\Phi_e \approx 3$ eV [22] (see figure 1(a)) and, hence, may be detected in the Al bottom electrode. A similar $\gamma - E_{pot}$ dependence as experimentally observed in the external electron emission is therefore comprehensible.

From the straight lines in figure 2 the tunneling yield induced by the potential energy γ/E_{pot} can be determined. For 1, 4, 8 and 12 keV, we find for γ/E_{pot} within an error of less than 10%: 9.5×10^{-4}, 9.7×10^{-4}, 9.6×10^{-4} and 9.4×10^{-4} e^- (ion $\cdot$ eV)$^{-1}$, respectively. Obviously, γ/E_{pot} is nearly independent of the kinetic energy of the projectile. This is again in good agreement with previous findings of external emission experiments. However, with a value of about 1×10^{-3} e^- (ion $\cdot$ eV)$^{-1}$, γ/E_{pot} is by about a factor of 10 smaller than the corresponding values γ_{ext}/E_{pot} measured in those experiments [16]–[18].

One reason for this difference between external and internal emission is that tunneling electrons have to cover larger distances within the solid than electrons ejected into the vacuum. In the energy range of 10–200 eV (corresponding to possible Auger transitions) the inelastic mean free path of electrons in silver is about 0.5–3 nm [23]. That means electrons traveling through the top Ag layer will undergo inelastic scattering processes before reaching the Ag–AlO_x interface, resulting in the creation of secondary electrons. The tunneling yield will be, therefore, the result of two competing effects: (i) an increase in the number of electrons having energies $E < \Phi_e$ and, hence, being unable to pass the oxide barrier and (ii) an overall increase in the number of excited electrons due to inelastic scattering.

It should be noted that holes excited in such Auger transitions may also be detected in the Al bottom electrode as a negative electron current, if they succeed to overcome the tunneling barrier with a mean height $\Phi_h \approx 4$ eV [24] (see figure 1(a)). Their energy is, however, restricted by the finite size of the conduction band. In addition, they have to overcome a higher barrier than electrons. As a consequence, the contribution of the holes to the tunneling yield at $U_{bias} = 0$ can be neglected.

Since γ depends approximately linearly on E_{pot} in this energy range, we can estimate a lower limit of the fraction of potential energy f_{int}, which is transported through the

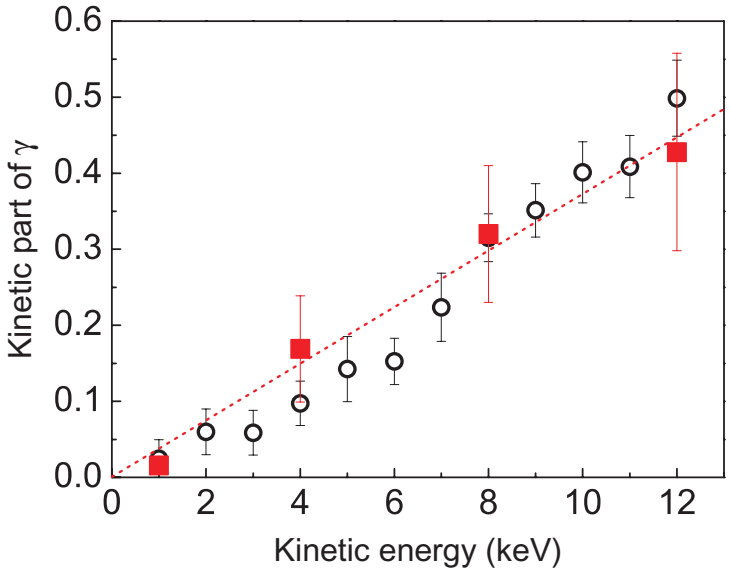

Figure 3. Kinetically induced internal emission yield versus kinetic impact energy of Ar projectiles for different charge states. Open circles represent scaled data (factor 2.5) for $q = 1$ taken from [25]. Full squares represent data obtained by extrapolation of the straight lines displayed in figure 2 to $E_{\mathrm{pot}} = 0$. The dotted line is an approximation to evaluate the efficiency of the kinetic energy to produce hot charge carriers.

oxide layer:

$$f_{\mathrm{int}} \geqslant \frac{\gamma \Phi_{\mathrm{e}}}{E_{\mathrm{pot}}} \approx 0.3\%. \tag{1}$$

The fraction f_{int} should also be by a factor of 10 lower than the fraction f_{ext} of potential energy transported into the vacuum. From external emission experiments [7] one finds, for instance, $f_{\mathrm{ext}}(q = 2) \approx 3\%$ and $f_{\mathrm{ext}}(q = 6) \approx 15\%$ which is in good agreement with our estimation of f_{int}.

The kinetic part of the internal electron emission yield can be determined by extrapolation of the straight lines drawn in figure 2 towards $E_{\mathrm{pot}} = 0$. The resulting values are displayed in figure 3 for the four different impact energies investigated here. Due to the fact that the four linear regression lines are parallel, the kinetic yield γ/E_{kin} appears to be independent of the actual projectile charge state q. This can be compared to the yield measured for singly charged ($q = 1$) projectiles [25][6], which are also included in figure 3. Note that the data of [25] were measured for an impact angle of 45° with respect to the surface. This results in a longer distance to the barrier and thus, in a reduced detection efficiency. Therefore, comparable yields with our data were obtained by multiplying the data from [25] by a factor of 2.5.

From figure 3 it appears as if in the energy range investigated here ($1\,\mathrm{keV} \leqslant E_{\mathrm{kin}} \leqslant 12\,\mathrm{keV}$) the kinetically induced tunneling yield exhibits an approximately linear dependence on the kinetic energy. From the dotted line in figure 3 one may estimate a yield of $\gamma/E_{\mathrm{kin}} = 0.37 \times 10^{-4}\,\mathrm{e}^{-}\,(\mathrm{ion}\cdot\mathrm{eV})^{-1}$. Note that this value is by more than one order of magnitude smaller than the potential yield ($\gamma/E_{\mathrm{pot}} \approx 1 \times 10^{-3}\,\mathrm{e}^{-}\,(\mathrm{ion}\cdot\mathrm{eV})^{-1}$) determined above. Apparently, the

[6] Note that the data presented in figure 3 (taken from [25]) slightly differ from those of [26]. As explained in detail in [25], this discrepancy was caused by an experimental artifact in our earlier data which was corrected in [25].

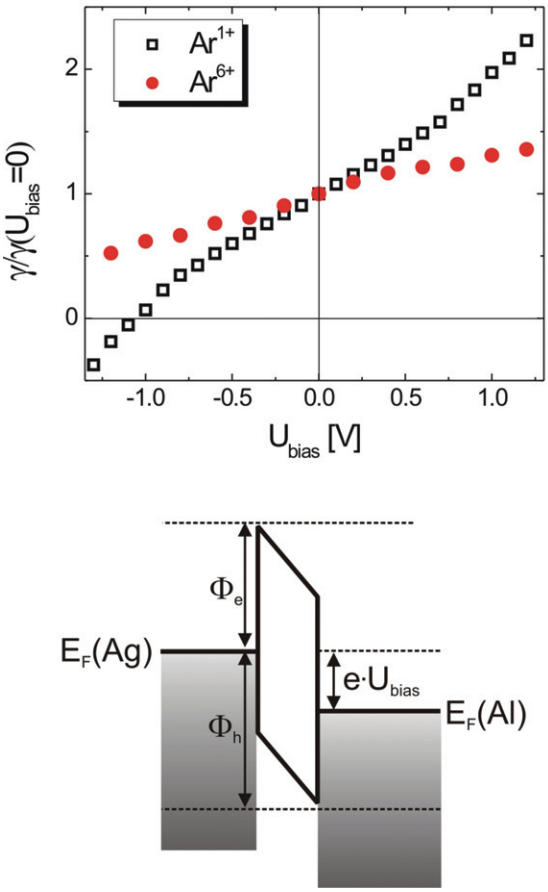

Figure 4. Upper part: measured internal emission yield as a function of bias voltage for two different charge states, i.e. Ar^{1+} (open squares) and Ar^{6+} (full circles). Lower part: schematic energy diagram for a biased MIM-junction (see figure 1(a) for comparison).

efficiency of kinetic energy to produce hot carriers capable of overcoming the tunnel barrier is much smaller than that of potential energy introduced into the surface.

In part, this difference can be rationalized by the fact that—for the energy range investigated here—the energy loss of an ion moving inside the metal is dominated by nuclear rather than by electronic stopping. However, target atoms set in motion by elastic collisions also experience inelastic energy loss to the electronic system. In fact, simulations show that more than half of the initial kinetic energy is transiently transferred to the electronic system within the first few picosecond after the projectile impact [27]. The vast majority of this energy, on the other hand, is stored in low-energy excitations, which do not contribute to the tunneling yield [28]. This situation is different for the potential energy carried by the MCI which predominantly generates high-energy excitations via Auger deexcitation processes. Hence, hot charge carriers produced by the dissipation of potential energy will be more likely to overcome the tunnel barrier.

A major strength of the MIM technique is the possibility to modify the characteristics of the tunneling junction by applying a bias voltage between the two metal layers. As sketched in the lower part of figure 4, this results in modified effective barrier heights and therefore changes

the relative detection efficiencies for hot electrons and holes. As a consequence, the balance between the contributions of both charge carriers to the net tunneling current is modified, leading to a strong bias voltage dependence of the measured internal emission yield. For singly charged projectiles ($q = 1$), this even leads to a polarity change of γ as shown in the upper part of figure 4.

Interestingly, the bias voltage dependence becomes much weaker with increasing projectile charge state ($q = 6$, full circles in figure 4). Again, this is due to the fact that the higher potential energy of the projectile generates more high-energy excitations. Since the maximum excitation energy of holes is in principle restricted to the Fermi energy, this leads to an asymmetry between the spectra of hot electrons and holes, rendering the hole contribution less important at higher projectile charge states. A detailed discussion of this effect is presented in a separate paper [13].

In conclusion, the results presented here demonstrate the applicability of MIM junctions as a novel tool to unravel the energy dissipation paths following the impact of MCI onto a metallic surface. Compared with external electron emission, the MIM provides complementary information on excitation states located below the vacuum level. We have demonstrated that by applying a bias voltage across the junction the tunnel barrier acts as an energy dispersive element. Hence, MIM junctions not only provide valuable information on yields of internal hot charge carriers excited by MCI impact, but can also be used to obtain further information on their spectral distribution.

Acknowledgments

Financial support by the DFG—SFB616: *Energy Dissipation at Surfaces* and by the European ITS LEIF network RII3#026015 is gratefully acknowledged.

References

[1] Gillaspy J D 2001 *J. Phys. B: At. Mol. Opt. Phys.* **34** R93
[2] Aumayr F, El-Said A S and Meissl W 2008 *Nucl. Instrum. Methods* B **266** 2729
[3] Briand J P, de Billy L, Charles P, Essabaa S, Briand P, Geller R, Desclaux J P, Bliman S and Ristori C 1990 *Phys. Rev. Lett.* **65** 159
[4] Meyer F W, Overbury S H, Havener C C, van Emmichoven P A Z and Zehner D M 1991 *Phys. Rev. Lett.* **67** 723
[5] Burgdörfer J, Lerner P and Meyer F W 1991 *Phys. Rev.* A **44** 5674
[6] Das J and Morgenstern R 1993 *Phys. Rev.* A **47** R755
[7] Kost D, Facsko S, Möller W, Hellhammer H and Stolterfoth N 2007 *Phys. Rev. Lett.* **98** 225503
[8] Grether M, Niemann D, Spieler A and Stolterfoht N 1997 *Phys. Rev.* A **56** 3794
[9] Schenkel T, Briere M A, Schmidt-Böcking H, Bethge K and Schneider D H 1997 *Phys. Rev. Lett.* **78** 2481
[10] Hattass M, Schenkel T, Hamza A V, Barnes A V, Newman M W, McDonald J W, Niedermayr T R, Machicoane G A and Schneider D H 1999 *Phys. Rev. Lett.* **82** 4795
[11] Arnau A *et al* 1997 *Surf. Sci. Rep.* **27** 113
[12] Schenkel T, Barnes A V, Niedermayr T R, Hattass M, Newman M W, Machicoane G A, McDonald J W, Hamza A V and Schneider D H 1999 *Phys. Rev. Lett.* **83** 4273
[13] Kovacs D A, Peters T, Haake C, Schleberger M, Wucher A, Golczewski A, Aumayr F and Diesing D 2008 *Phys. Rev.* B **77** 245432
[14] Diesing D, Kritzler G, Stermann M, Nolting D and Otto A 2003 *J. Solid State Electrochem.* **7** 389
[15] Galutschek E, Trassl R, Salzborn E, Aumayr F and Winter H P 2007 *J. Phys.: Conf. Ser.* **58** 395

[16] Arifov U A, Kishinevskii L M, Mukhamadiev E S and Parilis E S 1973 *Sov. Phys. Tech. Phys.* **18** 118
[17] Delaunay M, Fehringer M, Geller R, Hitz D, Varga P and Winter H 1987 *Phys. Rev.* B **35** 4232
[18] Kurz H, Aumayr F, Lemell C, Töglhofer K and Winter H P 1993 *Phys. Rev.* A **48** 2182
[19] Winter H 1992 *Europhys. Lett.* **18** 207
[20] Burgdörfer J J and Meyer F W 1993 *Phys. Rev.* A **47** 20
[21] Wentzel G 1927 *Z. Phys.* A **43** 524
[22] Kovacs D, Meyer S, Winter J, Wucher A and Diesing D 2007 *Phys. Rev.* B **76** 235408
[23] Ziaja B, London R A and Hajdu J 2006 *J. Appl. Phys.* **99** 33514
[24] Jennison D R, Schultz P A and Sullivan J P 2004 *Phys. Rev.* B **69** 41405
[25] Meyer S, Heuser C, Diesing D and Wucher A 2008 *Phys. Rev.* B at press
[26] Meyer S, Diesing D and Wucher A 2004 *Phys. Rev. Lett.* **93** 137601
[27] Duvenbeck A, Weingart O, Buss V and Wucher A 2007 *New J. Phys.* **9** 38
[28] Lindenblatt M, Pehlke E, Duvenbeck A, Rethfeld B and Wucher A 2006 *Nucl. Instrum. Methods* B **246** 333